

Soft-x-ray photoelectron, x-ray absorption, and autoionization spectroscopy of 1,5-cyclooctadiene on Si(001)-2×1

Florence Jolly, Fabrice Bournel, François Rochet,* and Georges Dufour

Laboratoire de Chimie Physique, UMR 7614, Université Pierre et Marie Curie, 11 rue Pierre et Marie Curie, F-75231 Paris Cedex 05, France

Fausto Sirotti and Amina Taleb

Laboratoire pour l'Utilisation du Rayonnement Electromagnétique, Centre Universitaire Paris-Sud, Bâtiment 209D, F-91405 Orsay Cedex, France

(Received 11 December 1998)

The adsorption of a nonconjugated diene, 1,5-cyclooctadiene, on Si(001)-2×1 is studied using valence-band and core-level soft-x-ray photoemission, near-edge x-ray absorption fine structure at the C 1s edge, and autoionization spectroscopy. Core-level spectroscopies validate the bonding model for room-temperature adsorption proposed by Hovis and Hamers [J. Phys. Chem. B **101**, 9581 (1997)]—based essentially on scanning tunneling microscopy (STM) and infrared spectroscopy experiments—where the diene attaches to the silicon surface via only one C=C bond. On the other hand, the complete quenching of the silicon surface states at saturation points to a coverage of one molecule per Si dimer, and not to a coverage of one molecule per two Si dimers, as the STM observation of locally 2×2 or *c*(2×4) ordered adsorption domains would suggest. The orientation of the free π orbital is deduced from the angular dependence of the C 1s absorption spectra. This orientational order is lost after thermal annealings of the molecular film (610–680 K range), before the molecule decomposes (at ~820 K). Valence-band spectra are taken at various photon energies (between 22 and 170 eV) to investigate the nature of the adsorbate-derived molecular levels resulting from the formation of the molecular film at 300 K. Valence-band spectra recorded at photon energies near the C 1s edge show that an electron promoted to the lowest unoccupied molecular orbital (π^*) of the chemisorbed molecule remains localized to the core-hole site, as both participator and spectator decay channels are observed.

[S0163-1829(99)12027-7]

I. INTRODUCTION

A fruitful association between organic chemistry and semiconductor surface science can be envisaged seriously since the recent discovery that ordered chemisorbed monolayers from *multiple functionality* hydrocarbons can be formed on a clean reconstructed Si(001)-2×1 surface.^{1,2} The experimental effort has been concentrated so far on the fundamental aspects of the reactivity of the silicon surface with molecules having two or more C=C double bonds.^{1,3–6} As a matter of fact, alkene groups, not involved in the bonding with the substrate, could be subsequently converted to other functional groups (alcohols, amines) or participate in polymerization reactions.

It is now well established that a simple alkene like ethylene (one C=C bond) attaches to the Si(001) surface via the interaction of the hydrocarbon π bond with the π bond of the Si dimer, producing two new Si—C bonds (the so-called di- σ bonding).⁷ This reaction is facile, and the sticking coefficient of the molecule at room temperature is close to unity, at least for coverages below one molecule per two Si dimers.⁸ In the formalism of organic chemistry, this reaction is termed a [2+2] cycloaddition, as a Si₂C₂ four-membered ring is formed. While there is a lack of clearcut experimental evidence pointing to the silicon dimer remaining intact, density functional theory calculations all point to an uncleaved silicon dimer.^{9–11}

However, the Si₂C₂ ring is strained, as a consequence of the difference between Si—Si (~2.35 Å) and C—C (~1.5 Å) bond lengths.

1,5-cyclooctadiene (1,5-COD) is a *nonconjugated* diene.¹² Its bonding to the silicon surface occurs necessarily via the [2+2] cycloaddition of one C=C double bond with one Si dimer, or of both C=C bonds with two adjacent Si dimers of a given dimer row. As a matter of fact, the distance between alkenelike bonds of gas phase *twisted-boat* 1,5-COD is indeed ~3.2 Å,^{4,13} a distance which nearly matches that of neighboring silicon dimers along a dimer row (3.8 Å). Using scanning tunneling microscopy (STM), Fourier-transform infrared (FTIR) spectroscopy, and x-ray photoelectron spectroscopy (XPS) (AlK α monochromatized source), Hovis and Hamers (Ref. 1) have investigated the interaction of 1,5-COD with the (001) surface. STM images show that for exposures of a few langmuirs (L) (1 L=10⁻⁶ Torr s) the molecules are aligned into rows, apparently in a unique bonding configuration. Molecules form ordered regions having local 2×2 or *c*(4×2) symmetry (the coverage would then be of one molecule per two silicon dimers). Hovis and Hamers find support from FTIR and XPS spectroscopies for their assumption of a molecule reacting only at one end, with the remaining alkene group exposed to the vacuum (this bonding configuration is depicted in Fig. 1). The (quasi) absence of infrared absorption peaks in the 2000–2150 cm⁻¹ Si-H stretching region points to an essentially nondissociative mo-

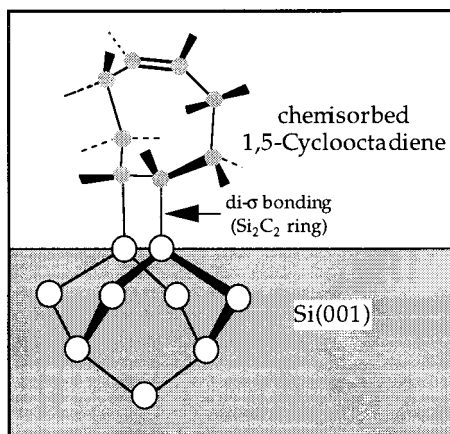


FIG. 1. Bonding geometry of 1,5-COD on the Si(001) surface according to Hovis and Hamers (Ref. 1).

lecular adsorption. The peaks observed in the 3020–3080 cm^{-1} region are attributed by the latter authors to CH alkene stretches: “at least some of the molecules [...] have bonded to the surface through only one double bond.” The XPS C 1s spectrum of a 1,5-COD-saturated surface (exposures are carried out at a substrate temperature of 50–100 °C) is reconstructed with a sum of three Gaussians at binding energies 283.7, 284.4, and 284.8 eV, assigned¹⁴ to carbon bonded to silicon (two atoms), alkanelike carbon (four atoms), and alkenelike carbon (two atoms), respectively, with intensities in the right proportion 1:2:1.

Synchrotron radiation core- and valence-electron spectroscopies, used in this study, shed light on many aspects of the adsorbate plus substrate system that are not attainable by vibrational spectroscopy or STM. First, the quenching of silicon surface states (both in valence-band and Si 2p core-level spectra) as a function of the exposure to the gas can be readily followed by synchrotron radiation x-ray photoemission (SRXPS), because of its high surface sensitivity. Second, near-edge x-ray absorption fine structure (NEXAFS) spectroscopy at the C 1s edge, which probes the carbon unfilled states having *p* symmetry, is able to detect the presence of specific bonds in the molecules (e.g., carbon-carbon π bonds via the observation of a $1s \rightarrow \pi^*$ resonance). Moreover, the resonance intensity associated with a specific molecular orbital (MO) final state is largest if the polarization vector \mathbf{E} of the radiation points in the direction of that MO, and the intensity vanishes if \mathbf{E} is perpendicular to the direction of that orbital. Consequently, it is possible to derive the spatial orientation of the MO final state.¹⁵ Third, autoionization and Auger spectra, taken at photon energies near the C 1s absorption edge, give information about the spatial localization of the unfilled adsorbate-derived orbitals. In the autoionization and Auger spectra we analyze electrons which are emitted due to the decay of the excited final-state x-ray absorption or x-ray photoemission processes, respectively. In the autoionization process we use a photon energy corresponding to the excitation of an electron to an initially unoccupied level. In single-particle terms, the excited state decays in two ways, denoted participator or spectator decay, producing different types of final states. In the participator decay the excited electron takes part in the decay process. The final

state is then a one-hole ($1h$) final state similar to the one in direct valence photoemission spectroscopy, and the two channels interfere with one another (resonant photoemission). If instead the excited electron remains as a spectator during the decay process the final state will be a two-hole one-particle final state ($2h1e$). On the other hand, the initial state for the “normal” Auger decay is the ionic final state after a photoemission process. During the decay one electron is emitted and another one fills the core hole. Hence the final state is a two-hole ($2h$) state. In a spectator decay the kinetic energy of the ejected electron is close to that of an ordinary CVV Auger electron, but is shifted to higher kinetic energy because of the screening effect of the spectator electron (the so-called “spectator” shift).

Our goals were (i) to examine the reaction of the silicon dangling bonds upon exposure to increasing doses of 1,5-COD at room temperature and, (ii) to validate, using core-level spectroscopies, the bonding model proposed by Hovis and Hamers, i.e., the diene bonds to Si dimers via only one C=C bond; (iii) to study the stability of the organic layer as a function of increasing annealing temperatures; and (iv) to determine by autoionization spectroscopy the spatial localization of the unfilled π^* orbital of the adsorbate. Points (iii) and (iv) are relevant to the functionalization issue of the surface, via thermal and photochemical processes, respectively.

This study is a part of our XPS/NEXAFS investigation series on the unsaturated hydrocarbon-Si interactions [Si(111)-acetylene,¹⁶ Si(001)-ethylene, and Si(111)-ethylene (Ref. 8)].

II. EXPERIMENT

A. Clean surface preparation and exposure to 1,5-COD

Si samples are prepared in an ultrahigh-vacuum (UHV) chamber whose base pressure is $\sim 10^{-10}$ Torr. The samples (phosphorus-doped silicon wafers, of resistivity 0.002–0.005 $\Omega \text{ cm}$) are heated by Joule effect (temperature measurements are made by infrared pyrometry). The silicon wafers are cleaned of their silica protective layer by heating at ~ 1520 K, in order to minimize SiC contamination.¹⁷ The surface cleanliness is checked by the intensity of the Si 2p core-level surface state, by a survey of the C 1s region (when energetically available), and by the sharpness of the low-energy electron diffraction (LEED) patterns characteristic of a two-domain 2×1 pattern.

Then the silicon surface is exposed to 1,5-COD—purified by several freeze-pump-thaw cycles—under pressures in the range 10^{-8} – 8×10^{-8} Torr, measured with an ionization gauge whose reading is not corrected. Exposures to the gas are given in langmuir units (see Table I).

B. X-ray photoemission

Photoelectron energy distribution curves are measured for valence bands (at $h\nu = 145$, 170, and around 285 eV), Si 2p (at $h\nu = 145$ eV), and C 1s (at $h\nu = 297.5$ and 330 eV) core levels with monochromatic synchrotron radiation delivered by the linear undulator of beam line SU7 of the SuperACO storage line. The undulator radiation is monochromatized by a 10-m TGM monochromator covering the 130–800 eV pho-

TABLE I. Durations, 1,5-COD pressures (uncorrected ion gauge reading), and corresponding exposures ($1 \text{ L} = 10^{-6} \text{ Torr s}$) to which the Si(001) surface are submitted at 300 K.

Time (s)	Pressure (Torr)	Dose (L)
50	10^{-8}	0.5
50	2×10^{-8}	1
100	2×10^{-8}	2
100	4×10^{-8}	4
100	8×10^{-8}	8
500	8×10^{-8}	40

ton energy range. A partially angle-integrating electrostatic electron energy analyzer (RIBER MAC2) is used. The linear polarization of the synchrotron radiation \mathbf{E} is at 40° to the axis of the cylindrical electron analyzer, defining a horizontal scattering plane. The sample surface is put in the common focus of the light beam and of the analyzer entrance lens and can be oriented about the vertical axis through the photoemission spot. The sample surface normal is always parallel to the analyzer axis and the light polarization vector is contained in the $(1\bar{1}0)$ plane of the Si(001) surface.

Additional valence-band spectra have been obtained at $h\nu = 22$ and 39 eV. Then the light source is the undulator of the high-resolution beam line SU3. The radiation is monochromatized by a PGM monochromator, upgraded to spherical mirror optics, covering the 5–250 eV photon energy range. The linear polarization of the synchrotron radiation \mathbf{E} is perpendicular to the $[001]$ direction of the silicon crystal and contained in the $(1\bar{1}0)$ plane. Photoelectrons are detected by an angle-resolved analyzer (VSW HAC150, angular acceptance $\sim 2^\circ$) at an angle of 45° from the normal to the sample surface. The overall energy resolution is about 40 meV.

The zero binding energy (the Fermi level E_F) is always taken at the leading edge of a clean metal surface (Ta or Cu) in electrical contact with the silicon crystal.

C. C 1s near-edge x-ray absorption fine structure spectroscopy

On beam line SU7, C 1s NEXAFS spectra of the adsorbed layer can be recorded at different angles θ between the normal to the sample surface and the polarization vector \mathbf{E} , in the range of 20° (grazing incidence) to 90° (normal incidence). The synchrotron polarization factor of the radiation is 100%, as the source is an undulator. The absorption is determined by collecting the total electron yield from the sample as a function of the photon energy. The detection consists of collecting electrons from the sample on an electron multiplier (dynode). We follow the same normalization procedure as in Ref. 16. We divide the spectrum of surface plus adsorbate by the spectrum of the clean surface alone. The energy resolution of beam line SU7 is about 550 meV at 285 eV. The absolute energy precision is estimated to ± 0.2 eV.

The NEXAFS spectrum of the molecular solid [a 1,5-COD multilayer deposited on a Pt(111) substrate held at liquid nitrogen temperature] has been obtained on beam line SA22, the energy resolution of which is about 100 meV at 285 eV.

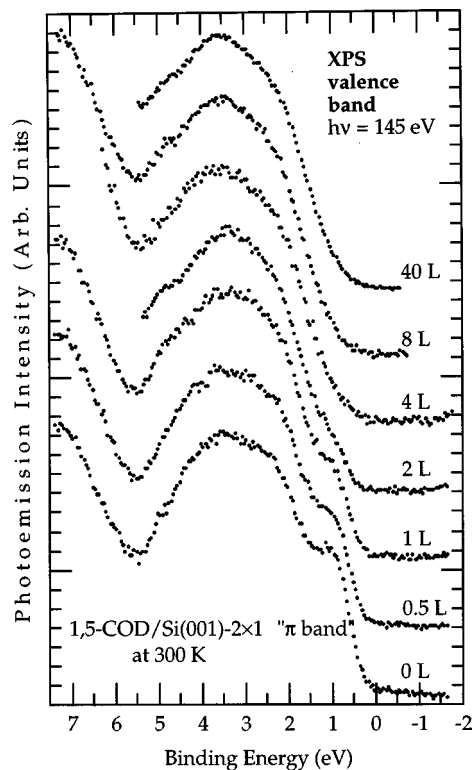


FIG. 2. Valence-band spectra of a Si(001)- 2×1 surface exposed to increasing doses of 1,5-COD at 300 K.

III. RESULTS AND DISCUSSION

A. How does the molecule bond on Si(001)- 2×1 ?

1. Chemisorption at room temperature

The valence band of the clean Si(001)- 2×1 , measured at $h\nu = 145$ eV, exhibits an intense surface state attributed to the occupied silicon dimer π band (see Fig. 2, bottom curve). [Although the surface sensitivity is not maximum at this photon energy, the observation of the silicon surface π band—when carbon is added to the surface—is easier than at $h\nu \sim 40$ eV (maximum surface sensitivity), simply because the calculated cross-section¹⁸ ratio of C 2p to Si 3p at $h\nu = 145$ eV is one order of magnitude smaller than at $h\nu = 40$ eV (see Table II).] The intensity of the surface state decreases gradually under exposure to 1,5-COD: practically, above 4 L, the silicon surface state is quenched. The so-called “outer dimer” states¹⁹ of the Si 2p core level exhibit

TABLE II. Photon energy dependence of the calculated photoionization cross-section ratios $\sigma(\text{Si } 3p)/\sigma(\text{Si } 3s)$, $\sigma(\text{C } 2p)/\sigma(\text{C } 2s)$, and $\sigma(\text{C } 2p)/\sigma(\text{Si } 3p)$ (Ref. 18).

$h\nu$ (eV)	$\sigma(\text{Si } 3p)/\sigma(\text{Si } 3s)$	$\sigma(\text{C } 2p)/\sigma(\text{C } 2s)$	$\sigma(\text{C } 2p)/\sigma(\text{Si } 3p)$
22	1.00	7	35
39.5	0.75	2	6.6
145	0.87	0.2	0.5
170	0.83	0.2	0.6
270	0.66	0.16	0.4
300	0.63	0.12	0.3

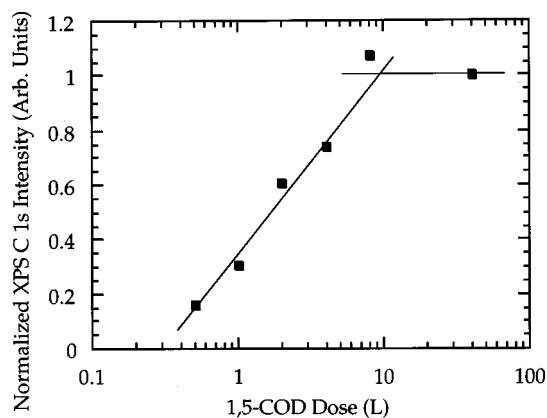


FIG. 3. C 1s photoemission intensity ($h\nu=330$ eV) versus 1,5-COD dose (L) to which the surface is exposed.

a similar quenching, while no feature related to the formation of the Si—C bond grows²⁰ (spectra are not shown). So far as the carbon uptake is concerned, it is monitored, by measuring at $h\nu=330$ eV, the C 1s peak intensity (Fig. 3). We note that C 1s intensity does not change appreciably from an exposure of 8 L. This saturation effect correlates well with the complete disappearance of the silicon surface states. However, the latter observation fails to agree with the description of the adsorbed layer at saturation given by Hovis and Hamers (Ref. 1), where molecules form locally a 2×2 or $c(2\times 4)$ reconstruction: *only half the surface dimers would then be consumed at saturation coverage.*²¹

Two typical C 1s spectra, corresponding to a 0.5 L exposure and a 40 L exposure, respectively, are given in Fig. 4. The spectra are reconstructed by the sum of only two Voigt curves. The low and high binding energy components, denoted respectively *L* and *H*, both have a full width of half maximum (FWHM) of 0.94 eV. For the 0.5 L exposure, *L* and *H* have binding energies at 284.3 and 284.9 eV, respectively, and intensitywise their ratio is 1:2. The overall shape of the peak does not change much with coverage. However, there is a measurable shift of the peak centroid towards higher binding energy (by ~ 0.25 eV) for the high coverages, maybe in relation to an increased stacking of the molecules. We have noted that, upon exposure to the gas, the energy position of the Si 2*p* bulk component does not shift by more than 0.05 eV, a value corresponding to the MAC2 spectrometer calibration uncertainty.

By decreasing the kinetic energy of the photoelectrons from ~ 45 eV ($h\nu=330$ eV) to ~ 12 eV ($h\nu=297.5$ eV) the escape depth is increased by a factor of about 3 or more.²² Assuming that the bonding model given in Fig. 1 is valid, at $h\nu=297.5$ eV ($h\nu=330$ eV) the measurement should be more sensitive to the innermost (outermost) carbon layer, which according to Hovis and Hamers (Ref. 1) should have the lowest (highest) binding energy. The plot (Fig. 5) of the C 1s spectra obtained at $h\nu=297.5$ and 330 eV shows they are identical. So, in contrast to the opinion of Hovis and Hamers (Ref. 1), we do not think that the asymmetric shape of the C 1s peak is simply due to the sum of components related to different chemical environments. Instead multi-electron effects or a vibrational fine structure [see also the C 1s spectrum of ethylene adsorbed on Si(001) which is also strongly asymmetric⁸] must be taken into account. In any

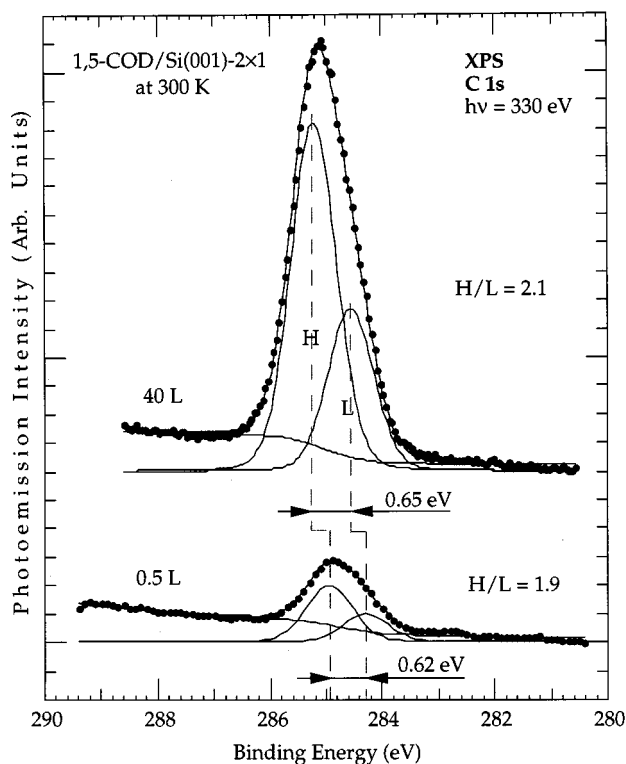


FIG. 4. C 1s photoelectron spectra (dots) of the Si(001) surface after exposures to 0.4 and 40 L of 1,5-COD at 300 K. Fits by a sum of two components (*H* and *L*) are also given (solid line). In each case, the Gaussian and Lorentzian FWHM are 0.9 and 0.1 eV, respectively. While the binding energy of the C 1s centroid shifts by ~ 0.25 eV at saturation, the energy distance between *H* and *L* and the intensity ratio *H/L* changes very little.

case C 1s XPS spectra do not evidence, nor exclude, the presence of alkenlike carbons.

On the other hand, NEXAFS spectroscopy gives direct evidence for the presence of alkene C=C bonds. We report the absorption spectra of solid 1,5-COD (the multilayer is formed at 80 K) and of the silicon surface exposed to 4 L of 1,5-COD at 300 K in Fig. 6. For the chemisorbed layer the ionization potential is at ~ 290 eV, taking the work function (4.8 eV) (Ref. 23) of the clean Si(001) surface. The transi-

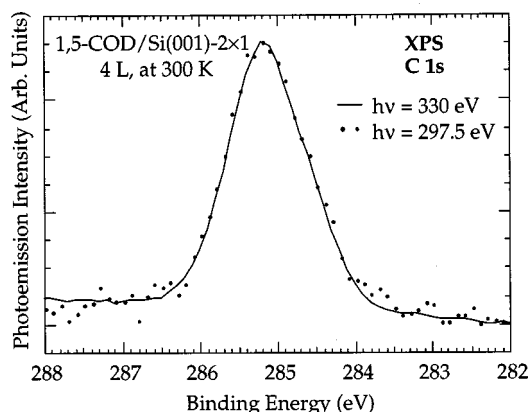


FIG. 5. C 1s photoelectron spectra taken at $h\nu=330$ and 297.5 eV (the secondary electron background is subtracted) of Si(001) exposed to 4 L of 1,5-COD at 300 K.

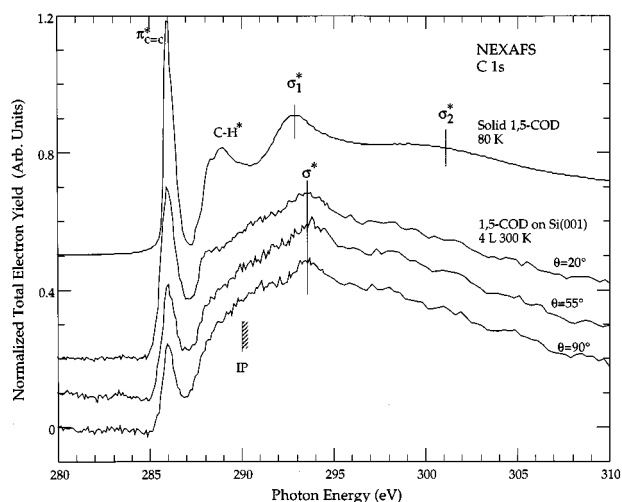


FIG. 6. C 1s NEXAFS spectra of solid 1,5-COD (80 K, beam line SA22) and of chemisorbed 1,5-COD on Si(001) (4 L, 300 K, beam line SU7). For the sake of peak position comparison the molecular solid spectrum is shifted down in energy by 0.4 eV. For the chemisorbed layer, the absorption curves are recorded at $\theta=90^\circ$ (\mathbf{E} parallel to the surface plane), $\theta=55^\circ$ (magic angle), and $\theta=20^\circ$ (\mathbf{E} close to the normal to the surface plane). The latter curves are normalized to an equal jump before the adsorption edge (275 eV) and ~ 80 eV after. For the chemisorbed molecule, the position of the ionization potential (IP) is given.

tions to bound states (i.e., below the ionization potential) are presented in more detail in Fig. 7. Let us first examine the NEXAFS spectrum of the molecular solid. Because the molecule is not π conjugated (i.e., the two C=C double bonds are far apart), we expect that the π system is not split into two π^* antibonding orbitals, as in butadiene, for example.²⁴ Indeed we observe a strong unique π^* resonance at 286 eV. The resonance at 288–289 eV is attributed to a C-H* transition. Two broad σ^* resonances at 293 and ~ 301 eV (denoted σ_1^* , σ_2^*) are also observed. The energy position of the first one is compatible with a single C—C bond; the second one at higher energy could be attributed to the shorter C=C bond, in the framework of the so-called “bond-length-with-a-ruler model.”²⁵ Alternately, as in the case of saturated rings or chains, the interaction between σ^* bonds may not be negligible and it may cause the splitting of the C-C σ^* resonance into two components.²⁶ The NEXAFS spectra of the solid compound remain unchanged when the angle θ between the radiation polarization vector \mathbf{E} and the normal to the substrate surface is varied (the molecules are randomly oriented).

Most of the NEXAFS spectral features of the molecular solid are retained in the case of the chemisorbed layer (4 L). By gently heating the substrate we have verified that a second layer of weakly bonded molecules is not adsorbed at room temperature after a 4 L exposure. Three resonances are observed, continuing the parent features (π^* , C-H*, and σ_1^*) of the molecular solid spectrum. In the case of a diene di- σ bonded to silicon via only one of the two C=C bonds, the other one remaining free, one expects in the π^* region the contribution of two components, one due to the free π^* orbital and one due to the second π^* orbital strongly hybrid-

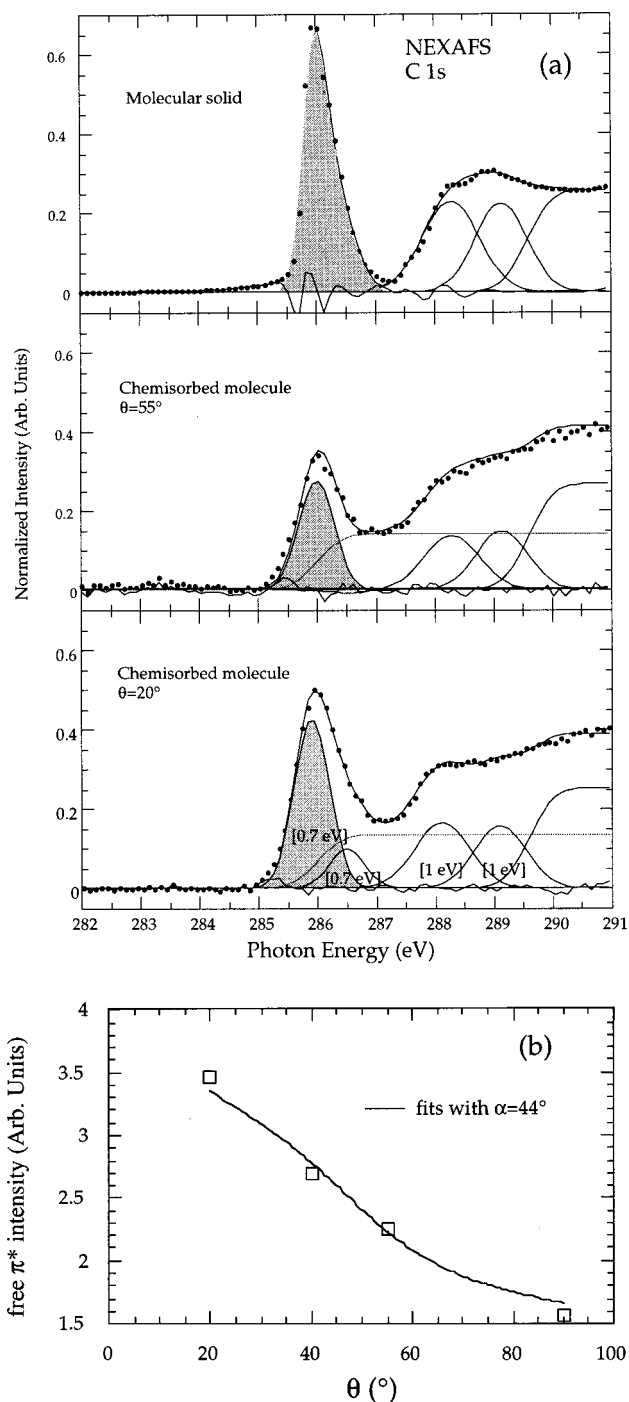


FIG. 7. (a) NEXAFS curve fits of the below IP region (molecular solid and chemisorbed layer). The figure illustrates the necessity for placing a “substrate” step (dotted) at ~ 286 eV in the case of the chemisorbed molecule and its absence in the case of the molecular solid. The vacuum level step (solid line) is placed at 289.7 eV. Both of them are simulated by step function convoluted by a Gaussian of FWHM 0.8 eV. All spectra are normalized so that the vacuum level height is equal. The π^* and C-H* resonances are simulated by sums of Gaussians (widths are given between brackets). The “free” π^* component is shaded in gray. With the normalization procedure used here, the ratio of the grayed areas (chemisorbed layer at magic angle)/(molecular solid), which is about ~ 0.44 , gives an estimate of the proportion of unreacted C=C double bond per molecule after adsorption, and hence confirms the model of Hovis and Hamers. (b) Determination of the free π^* orbital polar angle α from a fit of its intensity versus θ .

ized with silicon (C-Si*). In the case of ethylene (one C=C bond) the C-Si* state shows up in the NEXAFS spectrum as a weak shoulder before the C-H* peak,²⁷ and not as an intense white line. For chemisorbed 1,5-COD, the presence of a C-Si* line at higher photon energy [see Fig. 7(a)] than that of free π^* may account for the asymmetric shape of the resonance at 286 eV, but its precise intensity measurement is difficult, due to the presence of a step, corresponding to transitions to the densely spaced unfilled electronic states of the substrate having *p*-like symmetry. (Note the absence of such a step between the π^* and C-H* resonance in the molecular solid [Fig. 7(a)].)

In contrast with the case of the molecular solid, the NEXAFS spectrum of the chemisorbed molecule is modified when the incidence angle of the radiation is varied. As shown in Figs. 6 and 7(a), π^* intensity (and also C-H* intensity to a lesser extent) increases when the light approaches grazing incidences ($\theta=20^\circ$, i.e., \mathbf{E} close to the normal to the sample plane). On the other hand, σ^* intensity shows no dependence with θ . The symmetry of the silicon surface establishes several equivalent in-plane chemisorption geometries which lead to the formation of adsorbate domains. The actual clean Si(001) surface consists of terraces separated by monoatomic steps: the direction of the dimer rows (always aligned along a $\{110\}$ direction) is rotated by 90° from one terrace to the adjacent one. For an x-ray beam diameter (~ 1 mm) much larger than terrace dimensions, the technique samples many domains and the two-domain Si(001) surface has fourfold rotational symmetry about the surface normal. For threefold or higher symmetries, the π^* transition intensity I_π is

$$I_\pi \propto 1 + \frac{1}{2}(3 \cos^2 \theta - 1)(3 \cos^2 \alpha - 1), \quad (1)$$

where θ is the polar angle of \mathbf{E} and α is the polar angle of the vector final-state orbital.²⁸ The intensity of the “free” π^* orbital transition is measured following the procedure depicted in Fig. 7(a) (the area shaded in gray) and plotted against θ in Fig. 7(b). The best fit to relationship (1) is obtained for a π^* vector orbital making an angle of $\sim 44^\circ$ with respect to the sample normal. (Unfortunately the atomic positions resulting from the theoretical calculations of Ref. 1 are not given.)

We can now estimate, from an analysis of the NEXAFS spectra of the molecular solid and of the chemisorbed layer, how many C=C double bonds per molecule have, on the average, reacted with the Si dimers. First, we compare the molecular solid spectrum (the molecules are randomly oriented) to the chemisorbed molecule spectrum taken at the magic angle ($\theta=54.7^\circ$) for which the intensity distribution is indistinguishable from that of a random molecular orientation. Second, we have to find a good normalization procedure for which the same number of carbon atoms is taken into consideration. We note there are two steps (the substrate step at $h\nu \sim 286$ eV, and the vacuum level step at ~ 290 eV) for the chemisorbed molecule and only one step (the vacuum level step) for the molecular solid. As a consequence, the two experimental curves cannot be directly normalized to equal intensity jumps before the edge and well after the edge, as we have done for the angular series of spectra of the chemisorbed molecule. Instead the right normalization consists in

equating the vacuum steps of the molecular solid and of the chemisorbed molecule (at magic angle), determined by a fitting procedure [see Fig. 7(a)]. Then the ratio of the gray areas (chemisorbed molecule)/(molecular solid) is about 0.44. This measurement validates the model proposed by Hovis and Hamers in Ref. 1: one of the two initial C=C bonds does remain free after chemisorption of the molecule. Consequently, the complete quenching of the silicon surface states at saturation points to a maximum coverage of one molecule per *one* Si dimer, in contrast with the STM images of Ref. 1 which are indicative of a saturation coverage of one molecule per *two* Si dimers.²⁹ As a matter of fact, local *p*(2×2) or *c*(2×4) adsorbate superstructures have already been observed after alkene adsorption, more especially in the initial adsorption regime of ethylene (see Ref. 21). For ethylene, the strong reduction of the adsorption rate at a coverage of one molecule for two Si dimers implies that the molecule avoids dimer sites which are first neighbors of an already reacted site. Indeed a strong interadsorbate interaction at a coverage of one molecule per dimer has recently been evidenced by ultraviolet photoemission combined with theoretical calculations.¹¹ In the 1,5-COD case, although this molecule is bigger than ethylene, interadsorbate interactions at close-neighbor sites do not provoke a decrease of the adsorption rate.

2. Thermal stability

The thermal stability of the organic layer on Si(001)- 2×1 is studied by performing successive isochronal (1 min) annealings of a surface previously exposed to 4 L of 1,5-COD at room temperature. The SRXPS (C 1s and Si 2p) and NEXAFS spectra are recorded at room temperature after each annealing step. Heating at temperatures $T \leq 680$ K does not induce any change in the C 1s photoelectron spectral shape, apart from a downward binding energy shift of about 0.3 eV (Fig. 8). We note also a decrease in the peak intensity (-25%). No evidence for a desorption comes from the Si 2p or valence-band spectra (not shown) which do not exhibit the reformation of dimer surface states. The change in C 1s photoelectron intensity may come from a rearrangement of the molecules on the surface. This is suggested by the much more informative NEXAFS spectra (Fig. 9) which show that the π^* orbital broadens and loses its orientational order at 680 K. We note that the C-H* peak persists after the 610- and 680 K annealings, and is clearly visible. After the 820 K annealings, the C 1s photoelectron spectrum indicates that the molecule is certainly decomposed (two components at 284.7 and 283.4 eV show up). In contrast with the ethylene/Si system (Ref. 8) no incorporation of carbon in the silicon layers is observed at this temperature: the formation of the $\text{Si}_{1-x}\text{C}_x$ compound (with $x < 1$) would lead to the appearance of a component at a binding energy of 282.8 eV. Accordingly, the corresponding NEXAFS spectrum exhibits strong modifications. A product resulting from the decomposition of the molecule exhibits a (broad) π^* resonance which is strong at $\theta=20^\circ$ and almost killed at $\theta=90^\circ$, suggesting that the π^* orbital is oriented perpendicularly to the substrate.

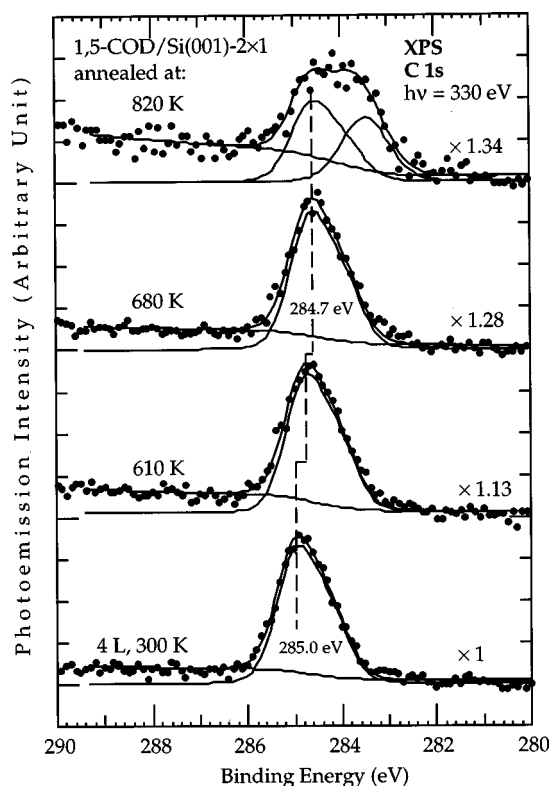


FIG. 8. C 1s photoelectron spectra of a 1,5-COD saturated surface (4 L at 300 K) and submitted to isochronal annealings (of 1 min each). The various spectra are multiplied by coefficients such that their areas, after background subtraction, are equal.

B. Photon energy dependence of valence-band photoemission and autoionization spectroscopy

Figure 10 shows the valence-band photoemission spectra of the Si(001) surface, saturated by 1,5-COD (at 300 K), which are recorded at photon energies 22 and 39.5 eV on beam line SU3, with an angle-resolved analyzer (the emission polar angle is 45°) and at 170 eV on beam line SU7, with a partially integrated analyzer. By comparing the spectrum of the dosed surface with that of the clean one, we note that the adsorbate-derived contribution to the valence band is made up of seven distinct features (from A to G). The adsorbate state density dominates over the silicon substrate contribution at low photon energy ($h\nu=22$ eV) for two reasons: (i) the photoelectron escape depth in silicon is close to a minimum, and thus the sensitivity to the adsorbate overlayer is high, and (ii) the ratio of the calculated photoionization cross sections (Ref. 18) for carbon $2p$ and silicon $3p$, $\sigma(C\ 2p)/\sigma(Si\ 3p)$, is around 35 (see Table II). Consequently the broad structure A (3–4 eV below E_F) and peaks B (at 6.8 eV) and C (at 8.9 eV) are adsorbate-related features. Structures A and B are essentially derived from C $2p$ orbitals, as they become undetectable at $h\nu=170$ eV [then the ratio $\sigma(C\ 2p)/\sigma(Si\ 3p)$ is only ~ 0.6]. Peaks D (13.1 eV), E (13.4 eV), F (15.8 eV), and G (18.3 eV), seen at the intermediate photon energy ($h\nu=39.5$ eV), with an intensity comparable to A and B, are the only carbon-derived states that can be observed at $h\nu=170$ eV. At this energy $\sigma(C\ 2s)$ is indeed an order of magnitude larger than $\sigma(C\ 2p)$. So we think that structures D–G are derived from C $2s$ orbitals.

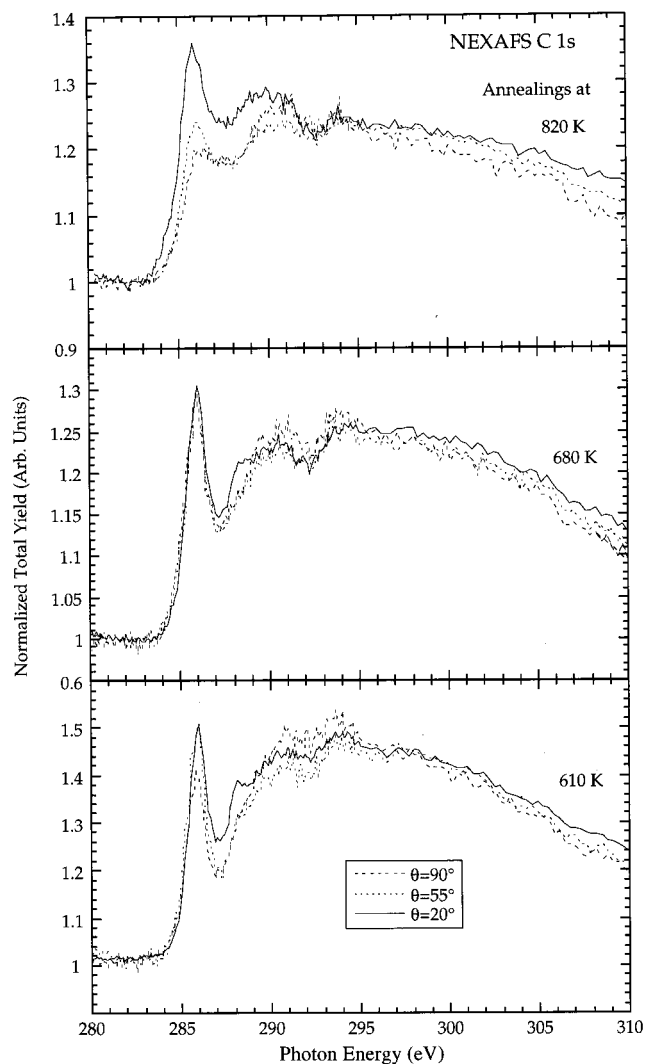


FIG. 9. C 1s NEXAFS spectra of a surface previously exposed to 4 L of 1,5-COD and submitted to isochronal annealings. The spectra are measured at three different polar angles θ , 90° (normal incidence), 55° (magic angle), and 20° (grazing incidence).

Structure C (9 eV) may be a mixed C $2s/2p$ component, as it is intense at $h\nu=22$ eV, and still present at $h\nu=170$ eV.

Table II shows that at still higher photon energy (in the 270–300-eV range) the contribution of carbon-derived states to the valence band should be extremely weak. This is indeed the case for spectra taken just before the C 1s edge (the π^* resonance stands at 286 eV), which are hardly distinguishable from those of the clean surface (apart from a C 1s photoemission peak excited by second-order light that may fall in the recorded energy range). The valence-band spectrum of a 4 L layer deposited at 300 K (recorded on beam line SU7), that is dominated so far by Si $3s$ and $3p$ emission, changes greatly for photon energies equal to or higher than the π^* resonance energy, i.e., when an electron is promoted from the C 1s core level into unoccupied adsorbate-derived orbitals (Fig. 6). In Fig. 11 we report valence-band spectra, normalized to the incident flux, obtained at photon energies bracketing the π^* resonance energy and at photon energies equal to or higher than the ionization potential (~ 290 eV), corresponding to transitions to continuum states. Then for

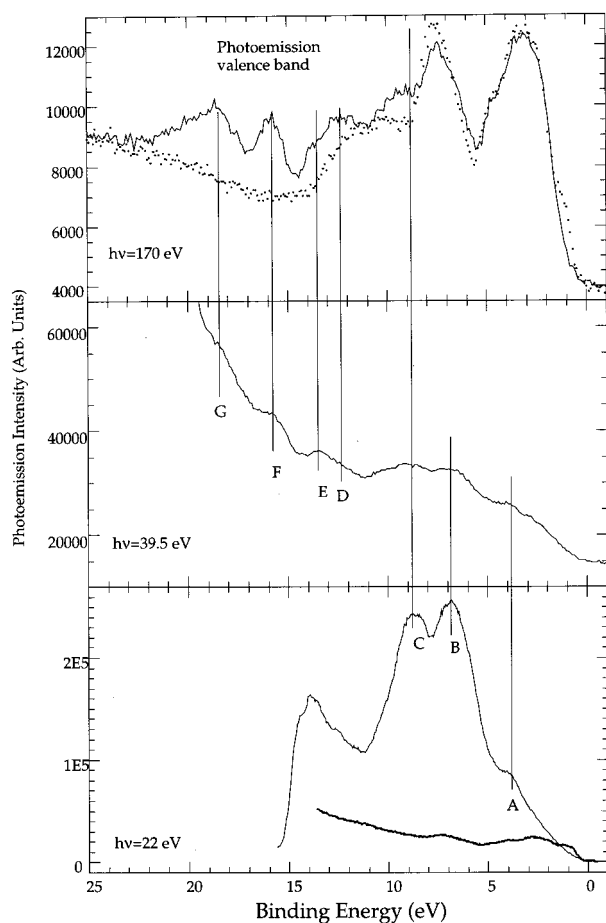


FIG. 10. Valence-band spectra of the Si(001) surface saturated by 1,5-COD at 300 K (solid line) and of the clean Si surface (dots). Measurements are made at various energies: $h\nu=22$, 39.5 (on beam line SU3), and 170 eV (on beam line SU7).

$h\nu \geq 286$ eV, each of the spectra shows a steplike feature which looks like an Auger decay. As recalled in the Introduction, at or near a resonance, the photoemission spectrum has three components: direct (normal) photoemission, participator (resonant channel) decay, and spectator decay (Auger-like). To remove the contribution of direct photoemission (silicon substrate plus adsorbate contributions), the nonresonant contribution (the dark solid curve in Fig. 11) obtained below the resonant energy (at 268 eV) is subtracted from the resonance spectrum (the second-order C $1s$ is also eliminated prior to subtraction). This operation makes sense because, in the photon energy range of interest (270–300 eV), the ratio $\sigma(\text{Si } 3p)/\sigma(\text{Si } 3s)$ varies smoothly (see Table II). The difference spectra corresponding to the resonant contribution are given in Fig. 12, plotted against a binding energy scale to better evidence the participator contribution [Fig. 12(a)], and against a kinetic energy to emphasize the spectator contribution [Fig. 12(b)]. A significant participator channel decay is only observed for photon energies near the π^* transition. It shows up in the 1–5 eV binding energy range: of the seven valence-band features (A–G) (see Fig. 10), only peak A (which has a C $2p$ character) is particularly enhanced: the corresponding orbital must have a similar spa-

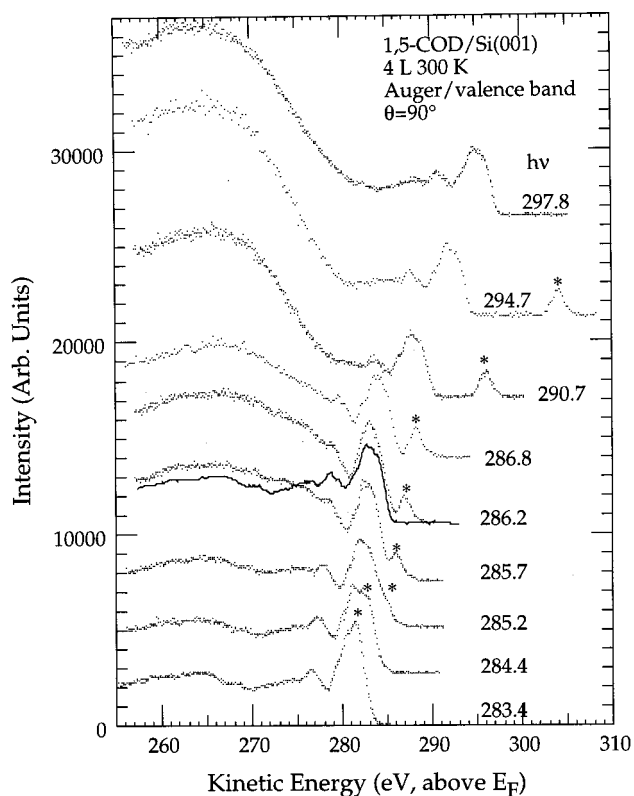


FIG. 11. Valence-band spectra (dots) of the Si surface (after exposure to 4 L of 1,5-COD at 300 K), obtained at photon energies around resonance C $1s \rightarrow \pi^*$, at photon energies close to the ionization threshold and above. The solid curve, superimposed to the 286.2-eV photon energy curve, corresponds to the direct photoemission contribution. Vertical scales are normalized with incident flux. The peaks marked with an asterisk (*) are carbon $1s$ core-level photoelectrons excited by second-order light.

tial extent to the π^* state, and comparable overlaps with the core hole to create an interference.

We have verified that from $h\nu=290.7$ eV (an energy close to the ionization threshold) to $h\nu=347$ eV the kinetic energy position of the Auger step does not vary. The dominance of “normal Auger” is indeed expected for continuum excitations.³⁰ In Fig. 12(b), the “normal Auger” spectrum of the adsorbate (denoted $2h$) is obtained by subtracting a valence spectrum measured at a photon energy below the $1s \rightarrow \pi^*$ resonance to the valence spectrum measured at the energy of 297.8 eV (Fig. 11). In the following, the shape of the spectator contribution to the valence band is taken to be that of the “normal Auger.” The “normal Auger” spectrum is multiplied by a scaling factor and shifted to higher kinetic energy to fit properly the step [the gray curve in Fig. 12(b) simulates the $2h1e$ step]. This “spectator shift” corresponds to the amount of screening due to the presence of the spectator electron in an orbital localized around the C $1s$ core-hole site. It amounts to about 3.8 eV at the energy of the C $1s \rightarrow \pi^*$ transition, for which the participator contribution is maximum [see Fig. 12(a)]. It decreases already to ~ 2 eV at a photon energy of 286.8 eV, for which the participator contribution is negligibly small [see Fig. 12(a)]. As indicated before, the spectator shift is already zero near the ionization

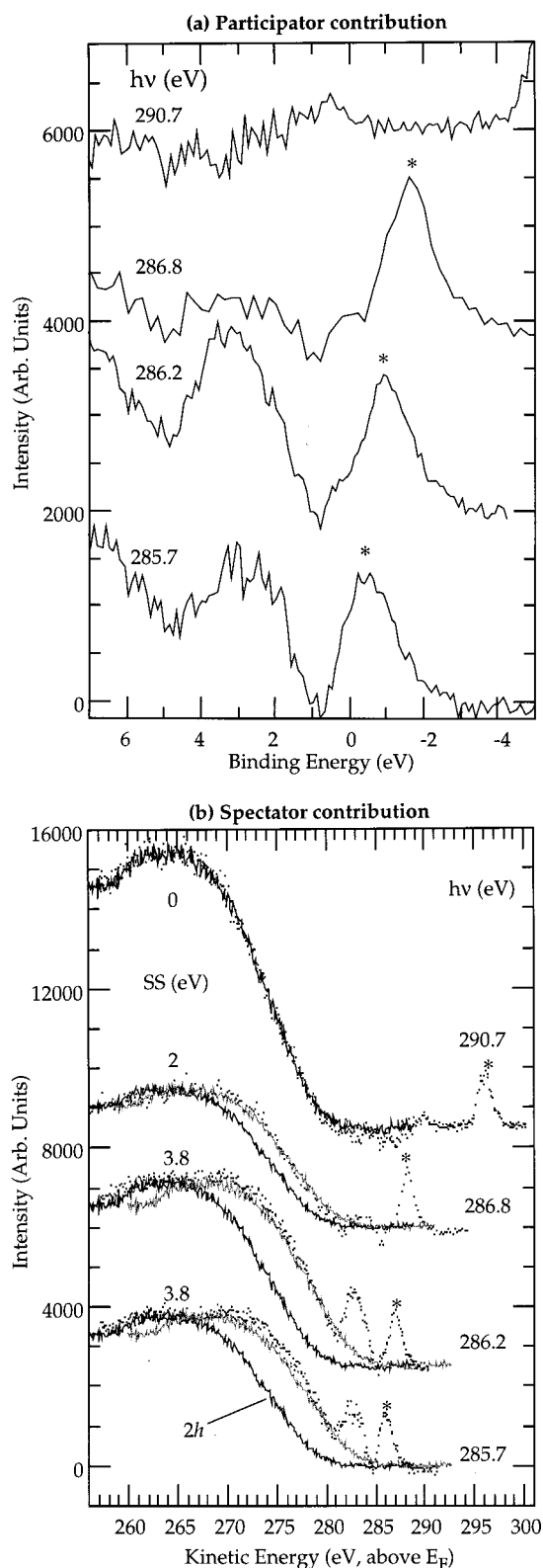


FIG. 12. Adsorbate autoionization spectra obtained after subtraction of the direct photoemission contribution, emphasizing (a) the participator channel (binding energy scale) and (b) the spectator channel. In (b), the normal $2h$ Auger is represented by a dark solid line. It is shifted to higher kinetic energy (gray line) by the spectator shift (SS) to simulate the $2h1e$ spectator contribution. In (a) and (b) the peaks marked with an asterisk (*) are carbon $1s$ core-level photoelectrons excited by second-order light.

threshold. The spectator shift results from the difference between the screening energy of the “normal” $2h$ Auger decay and that of the $2h1e$ spectator decay: in a simple electrostatic model, the screening energy of the former is three times as large as that of the latter (see Ref. 30). The spectator shift we find at the C $1s \rightarrow \pi^*$ transition (3.8 eV) is comparable to that found in the case of a condensed benzene ice layer (i.e., 3–4 eV, Ref. 30) or of a polystyrene film (2.9 eV, Ref. 31).

The observation of participator and spectator channels at the π^* resonance shows that an electron promoted into the π^* level remains localized around the C $1s$ core hole. Hopping to the substrate would be possible only if both the following conditions were fulfilled: first, the π^* orbital is coupled with the substrate, second, unoccupied Si states are energetically available. Undoubtedly the alkanelike carbons of the adsorbate act as a “spacer layer” between the free C=C double bond and the underlying substrate, reducing the possibility of charge transfer. Work is under way to examine the influence of the “alkane spacer” on the coupling with the substrate by using nonconjugated dienes (cyclic and linear) of various sizes.

IV. CONCLUDING REMARKS

The present paper discusses core-electron/valence-band photoemission spectra, absorption edge spectra, and autoionization spectra of 1,5-cyclooctadiene chemisorbed on Si(001)- 2×1 . Such spectra contain a wealth of information on this adsorbate/substrate system, which has been studied so far essentially by vibrational spectroscopies and topographic tunneling microscopy.

Upon adsorption at room temperature, the valence-band spectra show that the π bond of the Si dimers is destroyed, which is expected in the case of a di- σ bonding. At saturation we do not observe surviving surface states. The multi-component C $1s$ photoelectron spectrum does not produce proof of the existence of a free C=C bond. On the other hand, C $1s$ NEXAFS spectra, taken at various light incidence angles, demonstrate the presence of a π orbital, tilted by a polar angle of about 44° . By comparing the NEXAFS spectra of the molecular solid to those of a chemisorbed layer (4 L, 300 K), we estimate that, of the two initial C=C bonds, only one is involved in the bonding with Si dimers. Thus NEXAFS data fully validate the bonding model proposed by Hovis and Hamers (Ref. 1). As only one C=C bond per molecule reacts, and as all Si dimers are reacted at saturation, we infer a maximum coverage of one molecule per Si dimer, instead of one molecule per two Si dimers as shown by STM images (Ref. 1). The stability of the molecule is studied by performing thermal annealings of a chemisorbed layer. The crystalline order of the organic layer is certainly affected by annealings at moderate temperatures (610–680 K). At 820 K the molecule decomposes, but carbide-like compounds apparently do not form, in contrast with the case of small hydrocarbons deposited on silicon (see Ref. 8).

A very striking experimental result is the observation of a strong resonant enhancement to the valence band at the C $1s$ edge which recalls the resonances observed for a molecular solid (benzene) or a polymer (polystyrene).^{30,31} We find a

strong participator decay channel at the $C 1s \rightarrow \pi^*$ transition: the intensity of an adsorbate-derived valence orbital, of $C 2p$ character, is then resonantly enhanced. The spectator shift we measure compares with that found for solid benzene and polystyrene. It decreases when the photon energy approaches that of the ionization threshold and vanishes above. Participator and spectator decays are observed at the $C 1s \rightarrow \pi^*$ transition because the electron excited to the lowest unoccupied molecular orbital remains localized around the core-hole site.

Finally, in relation to the functionalization issue, we note that thermal treatments above room temperature may affect the order of the molecular layer, or even lead to its decom-

position. Low-temperature chemical reactions, induced selectively by photon irradiation at the $C 1s$ edge, could circumvent this difficulty. Indeed, photochemical reactions should be favored during spectator Auger transition, since the $C=C$ chemical bond is weakened by the excited electron remaining in the antibonding orbital.

ACKNOWLEDGMENTS

We warmly thank Dr. G. Panaccione, Dr. Ch. Grupp, Dr. C. Laffon, and Dr. Ph. Parent for their friendly help during all the measurements we made at Lure-SuperACO.

*Also at Laboratoire pour l'Utilisation du Rayonnement Electromagnétique, Centre Universitaire Paris-Sud, Bâtiment 209D, F-91405 Orsay Cedex, France. Author to whom correspondence should be addressed. Electronic address: roch@ccr.jussieu.fr

¹J. S. Hovis and R. J. Hamers, *J. Phys. Chem. B* **101**, 9581 (1997).

²J. T. Yates, Jr., *Science* **79**, 335 (1998).

³A. V. Teplyakov, M. J. Kong, and S. T. Bent, *J. Am. Chem. Soc.* **119**, 1110 (1997).

⁴A. V. Teplyakov, M. J. Kong, and S. T. Bent, *J. Chem. Phys.* **108**, 4599 (1998).

⁵J. S. Hovis and R. J. Hamers, *J. Phys. Chem. B* **102**, 687 (1998).

⁶J. S. Hovis, H. Liu, and R. J. Hamers, *J. Phys. Chem. B* **102**, 6873 (1998).

⁷J. Yoshinobu, H. Tsuda, M. Onchi, and M. Nishijima, *J. Chem. Phys.* **87**, 7332 (1987).

⁸F. Rochet, F. Jolly, F. Bournel, G. Dufour, F. Sirotti, and J. L. Cantin, *Phys. Rev. B* **58**, 11 029 (1998), and references therein.

⁹A. J. Fisher, P. E. Blöchl, and G. A. D. Briggs, *Surf. Sci.* **374**, 298 (1997).

¹⁰Wei Pan, Tianhai Zhu, and Weitao Yang, *J. Chem. Phys.* **107**, 3981 (1997).

¹¹U. Birkenheuer, U. Gutdeutsch, N. Rösch, A. Fink, S. Gokhale, D. Menzel, P. Trischberger, and W. Widdra, *J. Chem. Phys.* **108**, 9868 (1998).

¹²When *conjugated dienes* (1,3-dienes) react with silicon dimers, a second class of cycloaddition reaction, termed [4+2], can occur, leading to the formation of a larger, less strained Si_2C_4 six-membered ring. Although the theoretical calculation of Konecny and Doren [R. Konecny and D. J. Doren, *J. Am. Chem. Soc.* **119**, 11 098 (1997)] predicts that the [4+4] adduct is energetically more stable than the [2+2] one, a recent experimental work by Hovis *et al.* (Ref. 6) indicates (in contrast with Refs. 3 and 4) that the [2+2] addition is as facile as the [4+4] one. The formation of multiple products on the surface leads to a situation which is certainly not favorable for the growth of ordered organic layers on Si.

¹³W. R. Rocha and W. B. De Almeida, *J. Comput. Chem.* **18**, 254 (1997).

¹⁴C is more electronegative than silicon ($\Delta\chi=0.7$, see L. Pauling, *The Nature of the Chemical Bond*, 2nd ed. (Cornell University Press, Ithaca, NY, 1945). This should induce a charge transfer from Si to C. This change in charge would, *neglecting final-state contribution*, result in a lower ionization energy for the carbons bonded to silicon than for the alkanelike or alkenelike carbons of the chemisorbed molecule.

¹⁵J. Stöhr, in *NEXAFS Spectroscopy*, edited by R. Gomer, Springer

Series in Surface Science Vol. 25 (Springer-Verlag, Berlin, 1992).

¹⁶F. Rochet, G. Dufour, P. Prieto, F. Sirotti, and F. C. Stedile, *Phys. Rev. B* **57**, 6738 (1998).

¹⁷B. S. Schwartzentruber, Y.-W. Mo, M. B. Webb, and M. G. Lagally, *J. Vac. Sci. Technol. A* **7**, 2901 (1989).

¹⁸J. J. Yeh and I. Lindau, *At. Data Nucl. Data Tables* **32**, 1 (1985).

¹⁹E. Landemark, C. J. Karlsson, Y. C. Chao, and R. I. G. Uhrberg, *Phys. Rev. Lett.* **69**, 1588 (1992).

²⁰ $Si 2p$ features related to Si—C bond formation during alkene adsorption on Si cannot be detected with the overall resolution of beam line SU7 [see also the case of C_2H_4 adsorbed on Si(001) (Ref. 8)].

²¹In the case of C_2H_4 adsorption on Si(001)- 2×1 (Ref. 8), by correlating $C 1s$ intensity with $Si 2p$ and valence-band surface-state intensity, we had clear evidence for two regimes of adsorption: a rapid one (with a sticking coefficient close to unity) up to a carbon coverage of 0.5 monolayer (ML) (only half the silicon surface states were quenched), followed by a very slow regime (thousands of L were necessary to quench all surface states and saturate the surface). This was in agreement with STM observations of local 2×2 and $c(2 \times 4)$ superstructures up to exposures of about 6 L [A. J. Mayne, A. R. Avery, J. Knall, T. S. Jones, G. A. D. Briggs, and W. H. Weinberg, *Surf. Sci.* **284**, 247 (1993)].

²²M. P. Seah and W. A. Dench, *Surf. Interface Anal.* **1**, 2 (1979).

²³F. J. Himpsel, B. S. Meyerson, F. R. Mac Feely, J. F. Morar, A. Taleb-Ibrahimi, and J. A. Yarmoff, in *Proceedings of the Enrico Fermi School on "Photoemission and Absorption Spectroscopy of Solids and Interfaces with Synchrotron Radiation"*, edited by M. Campana and M. Rosei (North-Holland, Amsterdam, 1990), and references therein.

²⁴J. Stöhr, in *NEXAFS Spectroscopy*, edited by R. Gomer, Springer Series in Surface Science Vol. 25 (Springer-Verlag, Berlin, 1992), p. 186.

²⁵J. Stöhr, F. Sette, and A. L. Johnson, *Phys. Rev. Lett.* **53**, 1684 (1984).

²⁶J. Stöhr, in *NEXAFS Spectroscopy*, edited by R. Gomer, Springer Series in Surface Science Vol. 25 (Springer-Verlag, Berlin, 1992), p. 190.

²⁷F. Matsui, H. W. Yeom, A. Imanishi, K. Isawa, I. Matsuda, and T. Ohta, *Surf. Sci.* **401**, L413 (1998).

²⁸J. Stöhr, in *NEXAFS Spectroscopy*, edited by R. Gomer, Springer Series in Surface Science Vol. 25 (Springer-Verlag, Berlin, 1992), p. 284.

²⁹To explain this discrepancy, one could envisage that saturation

coverage was not attained in the STM work, after exposure of nominal 3 L, because of a different pressure calibration in Ref. 1 and in the present work.

³⁰D. Menzel, G. Rocker, H. P. Steinrück, D. Coulman, P. A. He-

imann, W. Huber, P. Zebisch, and D. R. Lloyd, *J. Chem. Phys.* **96**, 1724 (1992).

³¹J. Kikuma and B. P. Tonner, *J. Electron Spectrosc. Relat. Phenom.* **82**, 41 (1996).